

# Supramolecular Assembly Facilitating Adsorbate-Induced Chiral Electronic States in a Metal Surface

Nicolas Bovet,<sup>†</sup> Nicola McMillan,<sup>†,‡</sup> Nikolaj Gadegaard,<sup>‡</sup> and Malcolm Kadodwala<sup>\*,†</sup>

Department of Chemistry, Joseph Black Building, University of Glasgow, Glasgow G12 8QQ, U.K., and  
Department of Electronics and Electrical Engineering, Rankine Building, University of Glasgow,  
Glasgow G12 8LT, U.K.

Received: May 25, 2007; In Final Form: June 20, 2007

Through the application of optically active second-harmonic generation measurements (OA-SHG) we have demonstrated that the adsorption of amino acids cysteine ( $\text{HSCH}_2\text{CHNH}_2\text{COOH}$ ) and penicillamine ( $\text{HSC}(\text{CH}_3)_2\text{CHNH}_2\text{COOH}$ ) from solution can induce chiral electronic states in an initially achiral polycrystalline Au film. The chiral induction is strongly dependent upon the pH of the deposition solution; adsorption of penicillamine and cysteine under acidic conditions ( $\text{pH} = 3$ ) induces the same level of optical activity, whereas at  $\text{pH} = 11$ , the optical activity induced by cysteine is reduced by ca. 50% and penicillamine does not induce optical activity at all. The pH dependence indicates that the presence of interadsorbate hydrogen bonds, and consequently the supramolecular assembly of the adsorbates, facilitates the induction of chiral electronic states in the Au surface. This observation demonstrates that the symmetry properties of the extended structure of the self-assembled layer, and not the local adsorption geometry of the isolated adsorbed moiety, play the lead role in the induction of chiral metallic electronic states. The dependence of the chiral induction on COOH groups is identical to that observed in studies of optical activity in chiral thiol-protected nanoparticles, suggesting a common mechanism for the chiral perturbation in extended films and nanoparticles.

## Introduction

It is well-established that the electronic states of a metal ion can be chirally perturbed if it is placed in a chiral ligand environment; perhaps the best known example of this phenomenon is the circular dichroism (CD) in the metal–metal transitions, observed in the UV–vis region, of the  $\Lambda$  and  $\Delta$  isomers of  $[\text{Co}(\text{en})_3]^{3+}$ .<sup>1</sup> More recently, it has been demonstrated that noble metal nanoparticles grown in a chiral environment, such as that provided by chiral thiol protecting groups (e.g., cysteine and penicillamine)<sup>2–7</sup> or a DNA template,<sup>8</sup> have a chiral perturbation placed upon their electronic structure and consequently display optical activity. We have also shown recently that the adsorption of a chiral molecule can chirally perturb the surface electronic structure of a metal surface.<sup>9–11</sup> The induction of optical activity in atoms, nanoclusters, and extended surfaces is highly sensitive to the nature of the chiral environment. This is illustrated by studies which have shown that not all chiral protecting groups can induce optical activity in nanoparticles, induction of optical activity is facilitated by COOH groups,<sup>2–8</sup> and our own work, where not all chiral adsorbates induced a measurable chiral perturbation in the surface electronic structure of a metal.<sup>9–11</sup>

In an attempt to establish whether there is a connection between the induction of optical activity in nanoparticles and extended films we have studied the optical activity induced by the adsorption of penicillamine and cysteine on to a Au film. We have investigated whether the induction of optical activity in extended surfaces shares with cysteine/penicillamine-induced optical activity in nanoparticles the same dependence on COOH groups.

We have previously postulated that the ability of an adsorbate to convey chirality onto the electronic structure of a metal surface is related to its adsorption geometry. Specifically, an adsorbate can only chirally perturb the electronic structure of a metal if it adopts an adsorption geometry referred to as a “chiral footprint”, where at least three (noncollinear) inequivalent groups are in close proximity to the surface. This hypothesis is an application of the three points of contact rule, which is the classic way of rationalizing chiral interactions. In this study, we have obtained results that provide new insight into the mechanism by which adsorbates induce optical activity into a metal surface and reveal that the mechanism for chiral induction is more complex than we previously believed. We have demonstrated that amino acids penicillamine and cysteine can instill chiral electronic states in an initially achiral Au surface upon adsorption from solution, even though both of these molecules *do not* form adsorbed moieties that adopt chiral footprints,<sup>10</sup> that is, they interact with the surface with less than three points of contact. From the influence of the pH of the solution from which the amino acids were deposited, and the effects of the greater steric hindrance in the penicillamine overlayer, we have established that the induction of optical activity is strongly correlated to the symmetry properties of the self-assembled overlayers and not the local structure of the isolated adsorbed moieties. Induction of a chiral perturbation on the underlying metal surface is facilitated by the presence of significant interadsorbate interactions within an overlayer and the consequent formation of supramolecular assemblies, which produce overlayers with oblique lattices. When any chiral adsorbate, even those that do not have an individual chiral footprint, such as chemisorbed cysteine and penicillamine, are assembled into an ordered structure with an oblique lattice, the extended structure effectively displays a chiral footprint to the

<sup>†</sup> Department of Chemistry.

<sup>‡</sup> Department of Electronics and Electrical Engineering.

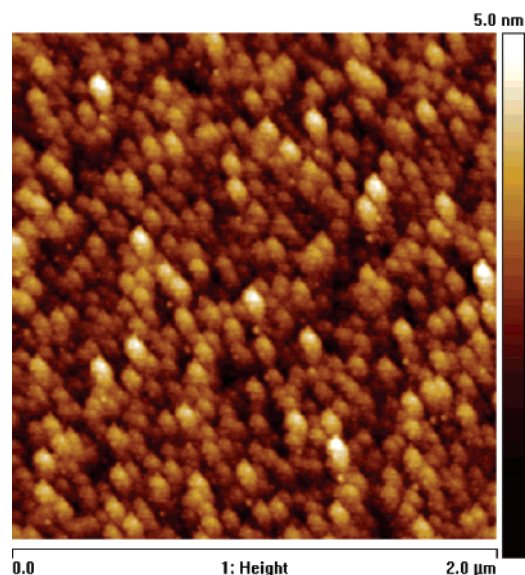


**Figure 1.** AFM image of the Au substrate prior to the adsorption of cysteine.

underlying substrate. It is the chiral footprint of the extended structure that chirally perturbs the underlying metal, and not the footprint of the isolated chemisorbed moieties.

### Experimental Section

The gold films used in this study were prepared by electron beam evaporation on silicon substrates. A 5 nm thick layer of titanium was evaporated as an adhesion promoter followed by 20 nm of gold without breaking the vacuum. Similar films have been used in studies of self-assembled monolayers (SAMs) of thiols.<sup>12</sup> The quality of Au films was monitored using atomic force microscopy (AFM) under ambient conditions; from the images obtained it was established that the films display a roughness of 0.6 nm, Figure 1. L- and D-Cysteine and penicillamine monolayers were deposited onto the Au film ( $\approx 1 \text{ cm}^2$ ) by immersion in 1 mM acidic (pH = 3) and basic solutions (pH = 11) for 18 h. The acidic conditions were produced by the addition of HCl, while basic conditions were the result of the addition of NaOH. For brevity we will refer to layers deposited from acidic and basic solutions as acidic and basic cysteine/penicillamine. After immersion, the films were rinsed with distilled water and dried in a stream of nitrogen gas. Each monolayer was formed on a freshly grown Au film.

Second-harmonic generation (SHG) measurements were performed using 8–12 ns pulses of fundamental Nd:YAG laser (Spectra Physics Quanta Ray) 1064 nm radiation at a repetition rate of 10 Hz and  $\sim 3.6 \text{ mJ/pulse}$ . The beam was defocused (10 mm diameter) and was incident on the crystal at  $60^\circ$  with respect to the surface normal; the incident polarization was varied using a  $\lambda/2$  plate. The SH signal (532 nm) was monitored at  $60^\circ$  with respect to the surface normal: it first passed through a polarizer before being focused into a spectrograph and then detected on an intensified CCD camera.

Two types of SHG measurements were performed in this study; in the first, the intensity of p-polarized SH radiation is monitored as a function of the polarization of the incident radiation. In the second, p-polarized radiation is incident on the surface and the SH intensity is monitored as a function of its out-going polarization. For brevity, these two experimental methodologies will subsequently be referred to as  $\text{pol}_{\text{in}}$  and  $\text{pol}_{\text{out}}$ . All profiles displayed are the average of five experiments collected from five freshly prepared surfaces.

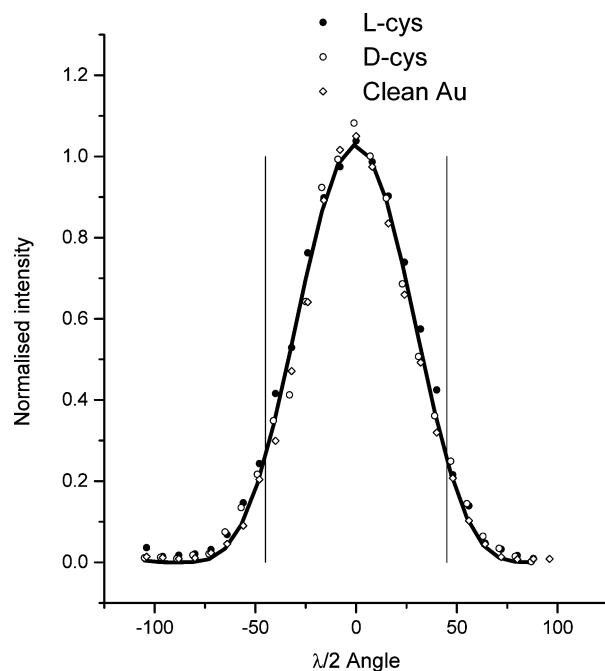


**Figure 2.**  $\text{Pol}_{\text{in}}$  profiles for a clean Au film (open diamonds), L-cysteine (filled circles), and D-cysteine monolayers (open circles) are shown, along with a best-fit  $\cos^4 \theta$  curve (solid line). The  $\lambda/2$  angle is defined as being relative to in-going p-polarized light. Solid lines are added to highlight the intensities at  $\pm 45^\circ$ .

### Results

Second-harmonic generation is an intrinsically surface sensitive probe of the electronic structure of an interface. The intensity of the SH signal is dependent upon the second-order susceptibility ( $\chi^2$ ) of the interface. For metallic interfaces the  $\chi^2$  is solely dominated by the contribution of the electronic structure of the metal; consequently, SHG monitors the adsorbate's induced perturbation of the electronic properties of the metal. In previous studies<sup>9–11</sup> we have demonstrated that optically active SHG (OA-SHG) is a highly sensitive probe to adsorbate-induced chiral perturbations of an initially achiral metal substrate. We now describe OA-SHG measurements from cysteine and penicillamine adsorbed on polycrystalline Au films.

**Clean Surface.** Profiles obtained from  $\text{pol}_{\text{in}}$  and  $\text{pol}_{\text{out}}$  experiments from a clean surface, Figures 2 and 3, have the same form as those reported in our previous study on a Cu(111) substrate;<sup>9–11</sup> they are symmetrical as would be expected for an achiral surface. The  $\text{pol}_{\text{in}}$  profile is fitted well with a  $I \propto \cos^4 \theta$  relationship. The  $\cos^4 \theta$  dependence of the SH signal reflects a quadratic dependence on the z-component of the intensity of the incident radiation. Such a dependence implies that the  $\chi_{zzz}$  component of the second-order susceptibility tensor is significantly larger than the other nonvanishing elements. The  $\text{pol}_{\text{out}}$  profile from the clean Au is once again symmetric and displays a reasonable fit with a  $\cos^2 \delta$  relationship. Such a  $\cos^2 \delta$  dependence is expected from a surface where the  $\chi_{zzz}$  is solely dominant. The dominance of the  $\chi_{zzz}$  element for the polycrystalline Au surface mirrors the behavior of other metal surfaces. Previous studies on Cu(111),<sup>9–11</sup> Pd(111),<sup>13</sup> Au(111),<sup>14</sup> Ag(111),<sup>14</sup> and Cu(110)<sup>15</sup> have shown that the  $\chi_{zzz}$  elements are at least 20 times larger than the next largest nonvanishing element.

**Cysteine and Penicillamine.** The immersion of the Au films in solutions (both acidic and basic) of either cysteine or penicillamine for 18 h results in an  $\approx 60\%$  reduction in SH signal (p-polarized in, p-polarized out). The significant reduction in SH signal after immersion is indicative of thiol adsorption. From

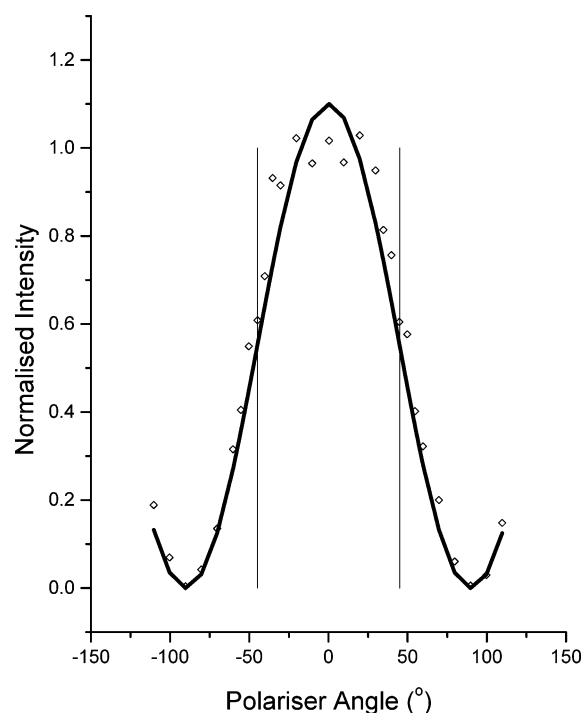


**Figure 3.**  $\text{Pol}_{\text{out}}$  profile for a clean Au film is shown. The polarizer angle is defined as being relative to p-polarized out-going light. The solid line is a best-fit  $\cos^2 \theta$  curve. Solid lines are added to highlight the intensities at  $\pm 45^\circ$ .

previous studies, it is known that thiol adsorption on Au leads to a decrease in SH signal intensity.<sup>16</sup> So similar levels of cysteine and penicillamine adsorption onto the Au substrate occur in both acidic and basic solutions.

As in our previous studies of chiral monolayers on metal substrates, the  $\text{pol}_{\text{in}}$  profiles, Figure 3, collected from the four chiral monolayers studied display no measurable asymmetry. The  $\text{pol}_{\text{out}}$  profiles for both enantiomers of the four chiral monolayers are displayed in Figures 4 and 5; a detailed description of the analysis of the profiles can be found elsewhere.<sup>10</sup> The asymmetry of the profiles have been parametrized using the  $I_{45}/I_{-45}$  and  $I_{-45}/I_{45}$  ratios, Table 1. An optically active response would result in the  $I_{45}/I_{-45}$  for one enantiomer being equal to the  $I_{-45}/I_{45}$  ratio of the other. From inspection of Figures 4 and 5 it appears that the profiles from acidic solutions of penicillamine and cysteine are more asymmetric than those obtained under basic conditions. The less asymmetric nature of the basic cysteine and penicillamine profiles is confirmed by the  $I_{45}/I_{-45}$  and  $I_{-45}/I_{45}$  ratios in Table 1. The  $I_{45}/I_{-45}$  and  $I_{-45}/I_{45}$  ratios for the four basic L- and D-cysteine and penicillamine profiles are all closer to unity than the four acidic profiles, implying a smaller asymmetry than the corresponding acidic values. The basic L- and D-cysteine values display a small asymmetry, whereas the D- and L-penicillamine profiles display no asymmetry within experimental error.

## Discussion

The OA-SHG measurements clearly demonstrate that both acidic cysteine and penicillamine can induce optical activity in the surface electronic structure of an initially achiral Au surface. The data also clearly demonstrates that the induction of optical activity is sensitive to the pH of the deposition solution, with acidic conditions facilitating the induction of optical activity. The similar levels of reduction in the SH signal upon deposition

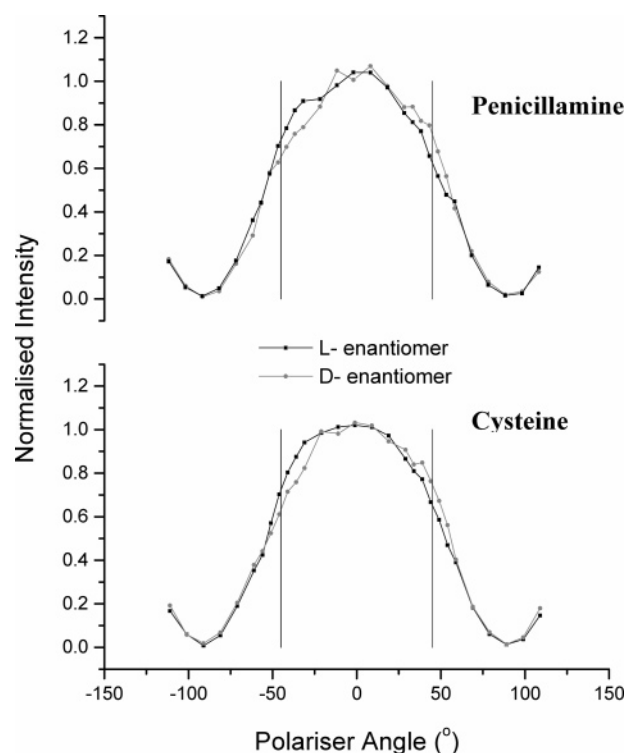


**Figure 4.**  $\text{Pol}_{\text{out}}$  profiles for acidic cysteine and penicillamine are shown; angles are defined as being relative to out-going p-polarization. Solid lines are added to highlight the intensities at  $\pm 45^\circ$ .

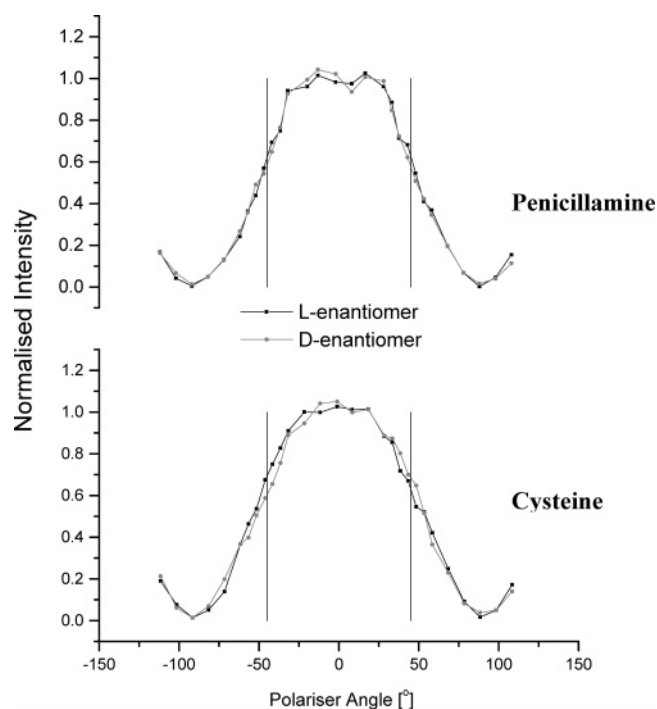


**Figure 5.**  $\text{Pol}_{\text{out}}$  profiles for basic cysteine and penicillamine are shown; angles are defined as being relative to out-going p-polarization. Solid lines are added to highlight the intensities at  $\pm 45^\circ$ .

from acidic and basic conditions demonstrates that, as expected, surface coverage is insensitive to the pH of the deposition solution. The second important observation is that although there is no difference in the levels of optical activity induced by cysteine and penicillamine for acidic conditions, there is a discernible difference in the basic data, with penicillamine adsorption inducing no detectable optical activity, indicating that steric hindrance plays a role under basic conditions.



**TABLE 1: Asymmetry Parameters for the Cysteine and Penicillamine Layers<sup>a</sup>**

	acidic pH = 3		basic pH = 11	
	$I_{45}/I_{-45}$	$I_{-45}/I_{45}$	$I_{45}/I_{-45}$	$I_{-45}/I_{45}$
D-cysteine	$0.90 \pm 0.03$	$1.11 \pm 0.03$	$0.94 \pm 0.03$	$1.06 \pm 0.03$
L-cysteine	$1.17 \pm 0.03$	$0.85 \pm 0.03$	$1.10 \pm 0.03$	$0.91 \pm 0.03$
D-penicillamine	$0.85 \pm 0.03$	$1.18 \pm 0.03$	$1.00 \pm 0.03$	$1.00 \pm 0.03$
L-penicillamine	$1.18 \pm 0.03$	$0.85 \pm 0.03$	$1.00 \pm 0.03$	$1.00 \pm 0.03$

<sup>a</sup> The stated errors are derived from the standard deviation of the ratio obtained from five profiles.

The first step in understanding the origin of this pH dependence of the induction of optical activity is a discussion of the structures of the overlayers formed under acidic and basic conditions. In the subsequent discussion, we will concentrate on studies that have been performed on the (111) face of Au. The (111) face of Au is the thermodynamically most stable low-index face and the one that will predominate in polycrystalline films, such as those used in the current study. Consequently, the phenomena observed in studies on (111) faces of Au will also dominate the behavior of the polycrystalline sample used in our study.

There is a large body of work concerning the structure of cysteine adsorbed under a variety of deposition conditions (gas phase, from solution, and under electrochemical conditions). In contrast there has been little work on penicillamine/Au interfaces; however, it is our assertion that the behavior of penicillamine will be qualitatively similar to that of cysteine; consequently, arguments made for the structure of cysteine are equally valid for penicillamine.

**pH Dependence on the Moieties Formed by Chemisorption.** Depending upon pH, amino acids can exist as anionic, cationic, and zwitterionic forms in solution; in a similar manner, chemisorbed cysteine deposited from solution can also adopt these forms. Based on IR spectroscopy measurements Ihs and Liedberg,<sup>17</sup> tentatively suggested that when deposited from pH 1.5 and unbuffered (pH 5.7) solutions a cationic chemisorbed cysteine species,  $-\text{SCH}_2\text{CH}(\text{COOH})\text{NH}_3^+$ , was formed with its  $\text{NH}_3^+$  group in the vicinity of the surface, while the  $\text{COOH}$  group pointed away from it. In contrast, under basic conditions cysteine adsorption leads to the formation of a chemisorbed anionic moiety,  $-\text{SCH}_2\text{CH}(\text{COO}^-)\text{NH}_2$ , and it was suggested that the  $\text{NH}_2$  group of the species coordinated to the Au surface, while its  $\text{COO}^-$  pointed away from it. Ihs and Liedberg also speculated that the  $\text{Na}^+$  from the NaOH used to produce the basic conditions coordinated to the carboxylate group.

In a recent study Gonella et al.<sup>18</sup> have been able to determine quantitatively, using O(1s) XPS, the amount of  $\text{COOH}$  groups which remain protonated within a chemisorbed cysteine layer deposited from a solution of pH 5.7. They were able to quantify the fraction of carboxylic acid groups deprotonated because the oxygen atoms within the carbonyl ( $\text{COOH}$ ), hydroxyl ( $\text{COOH}$ ), and carboxylate ( $\text{COO}^-$ ) groups have characteristic binding energies of  $532.3 \pm 0.2$ ,  $533.6 \pm 2$ , and  $531.2 \pm 2$  eV. Through peak fitting the O(1s) spectra it was established that ca. 30% of the carboxylic acid groups within the layer remained protonated. We have also collected O(1s) spectra from cysteine deposited from an acidic, pH = 3, Figure 6, solution to determine the amount of deprotonation (we have also collected C(1s) and S(2p) XPS data which is similar to that of Gonella et al., see the Supporting Information). Our spectra could be fitted to identical components to those used by Gonella et al. ( $531.4 \pm 0.2$ ,  $532.1 \pm 0.2$ , and  $533.6 \pm 0.2$  eV). Our O(1s) spectrum is consistent with 66% of the carboxylic acid groups remaining protonated.

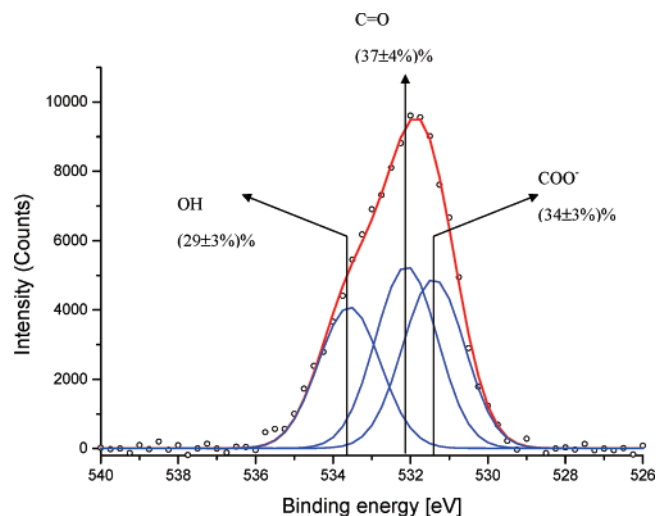


**Figure 6.** O(1s) spectrum collected from a cysteine/Au layer deposited from a solution of pH = 3. The spectrum has been fitted with three components associated with OH, C=O, and  $\text{COO}^-$  groups. The relative contribution each component makes to the overall fit (with associated error) is given. Binding energy is calibrated against the Au  $4f_{5/2}$  peak.

This fraction is larger than that observed by Gonella et al. and is consistent with the more acidic nature of the deposition solution used in our work (pH 3 compared to 5.6).

In summary, from our own measurements and those by other groups in previous studies, we can state that under the acidic conditions used in our study, pH of 3, a significant fraction of chemisorbed cysteine, and by inference penicillamine, will retain intact carboxylic acid groups.

**Local Structure of the Chemisorbed Thiols.** Until recently, it was believed that chemisorbed thiols, including cysteine and penicillamine, adsorbed so that the sulfur atom occupied threefold hollow sites.<sup>19</sup> However, Yu et al. have established that this simple view of the thiol local registry is incorrect in a recent structural study, supported by theory.<sup>20</sup> They determined that upon thiol adsorption, mobile  $\text{Au-S-R}$  moieties are formed. The existence of these mobile  $\text{Au-S-R}$  moieties also helps to explain the significant reconstruction of Au surfaces induced by thiols including cysteine.<sup>21</sup> Scanning tunneling microscopy (STM) images taken after the adsorption of cysteine on Au surfaces reveal that they display significantly more roughness than prior to adsorption, with the etching of steps and the formation of monolayer deep pits; this etching behavior is ubiquitous among thiols.<sup>19</sup> Such a considerable reconstruction of the surface requires a significant amount of adsorbate-facilitated mass transport. The extraction of Au atoms from terrace and step sites by the adsorbed thiols to form the  $\text{Au-S-R}$  moieties would explain the observed reconstruction.

**Self-Assembly of Cysteine.** Adsorbed cysteine, like other thiols, can self-assemble and produce a range of well-ordered overlayer structures on Au surfaces.<sup>21–25</sup> Self-assembly of cysteine/penicillamine overlayers, like any adsorbate, is governed by the interplay between adsorbate–adsorbate and adsorbate–substrate interactions. In the case of cysteine/penicillamine the interadsorbate interactions will be governed by the forms of cysteine/penicillamine existing within the overlayer, specifically whether they are anionic, cationic, zwitterionic, or neutral. This can be directly influenced by the pH of the deposition solution. In the case of the anionic and zwitterionic forms, only electrostatic forces will operate within the overlayer. However, for the other forms intermolecular

**TABLE 2: Ordered Structures Observed for Cysteine on Au(111)**

structure	no. of molecules per unit cell	condition	Bravais net
$\sqrt{3} \times \sqrt{3}$ R30° <sup>a</sup>	1	zwitterionic	hexagonal
$3\sqrt{3} \times 6$ R30° <sup>b</sup>	6	acidic pH = 4.6	oblique
$4 \times \sqrt{7}$ R19° <sup>c</sup>	2	acidic pH = 1	oblique

<sup>a</sup> Refs 21 and 24. <sup>b</sup> Refs 22 and 25. <sup>c</sup> Ref 23.

hydrogen bonds, which in contrast to electrostatic interactions are unidirectional, will influence structure.

The effects of hydrogen bonding and electrostatic interactions on the self-assembly of cysteine/penicillamine on Au surfaces is illustrated in previous work performed on single-crystal surfaces.<sup>21–25</sup> The self-assembly of cysteine on the (111) face has been most extensively studied, Table 2. It is important to note that this work clearly shows that domains of a variety of phases can coexist on a surface and that the nature of the ordered structures formed depended significantly on deposition conditions/method. In an early STM study, Dakkouri and co-workers<sup>21</sup> adsorbed cysteine directly from an aqueous solution finding that the adsorbed cysteine was predominantly in the zwitterionic form and produced a  $\sqrt{3} \times \sqrt{3}$  R30° structure. Such a structure was also observed when cysteine was deposited onto gold from the gas phase.<sup>24</sup> The  $\sqrt{3} \times \sqrt{3}$  R30° is a “classic” structure for self-assembled layers of alkyl thiols.<sup>19</sup> In more recent STM studies performed under acidic conditions domains of more complex structures,  $3\sqrt{3} \times 6$  R30°<sup>22,25</sup> and  $4 \times \sqrt{7}$  R19°<sup>23</sup> have been observed.

In the case of the  $\sqrt{3} \times \sqrt{3}$  R30° structure, Figure 7, the adsorbate–substrate interaction dominates producing an ordered structure which retains the hexagonal lattice of the underlying substrate, although the presence of the asymmetry center in the chiral thiol lifts the mirror symmetry of the surface. In contrast, there are significant adsorbate–adsorbate interactions in the two complex phases, specifically, intermolecular hydrogen bonding involving the COOH groups. The  $4 \times \sqrt{7}$  R19° and  $3\sqrt{3} \times 6$  R30° phases contain hydrogen-bonded supramolecular assemblies of two and six cysteine moieties, respectively; the  $3\sqrt{3} \times 6$  R30° is shown in Figure 7. The presence of interadsorbate interactions, such as hydrogen bonding, produces an overlayer that has significantly different symmetry properties to the Au substrate; not only is the mirror symmetry lifted by the asymmetric center of the adsorbate, but the adsorbate–adsorbate interactions produce a structure which has an oblique rather than a hexagonal Bravais net, with twofold rather than sixfold rotational symmetry.

**The Origin of the pH Dependence of the Induced Optical Activity.** We believe that the pH dependence of the chiral induction can be explained by the different symmetry properties of the cysteine/penicillamine overlayers formed under acid and basic conditions. Under basic conditions the likelihood of supramolecular assembly is reduced because of the absence of intermolecular hydrogen bonding, with only nondirectional electrostatic interactions driving supramolecular assembly. Consequently, it is more likely that structures will be formed that, like the  $\sqrt{3} \times \sqrt{3}$  R30°, retain the hexagonal lattice of the bare surface. The retention of the hexagonal lattice of the bare substrate in the chiral self-assembled layer has an important effect. This is illustrated using the  $\sqrt{3} \times \sqrt{3}$  R30° structure, Figure 7, which belongs to the space group *p6*. If one considers the structure formed by the Au atoms that are part of the Au–cysteine moiety, they form a hexagonal structure, which in the absence of the cysteine group would have mirror symmetry,

and belong to space group *p6mm*. In contrast, for the oblique lattices of the supramolecular structures of, for example,  $3\sqrt{3} \times 6$  R30°, which belongs to space group *p1*, the Au atoms still have an intrinsically chiral structure (still with a space group *p1*) in the absence of the asymmetric center of the adsorbate.

So the induction of a chiral perturbation on the surface electronic structure is dependent upon the supramolecular assembly of the adsorbed cysteine/penicillamine moieties. The steric effect observed under basic conditions can be readily understood in terms of the proposed model. The nondirectional nature of electrostatic interactions means that they are less efficient at producing ordered surface supramolecular assemblies, hence the reduced level of asymmetry for basic cysteine. The less effective nature of electrostatic interactions for producing ordered supramolecular assemblies also means that they will be more susceptible to the extra steric hindrance of the two methyl groups on the  $\alpha$ -carbon of the penicillamine. In contrast, under acidic conditions the two methyl groups on the  $\alpha$ -carbon of the penicillamine do not obstruct the COOH group and consequently have little influence on the interadsorbate hydrogen bonds.

A point we wish to address is the smaller levels of optical activity displayed by the penicillamine/cysteine/Au interfaces compared with those observed in our previous study of 1-(1-naphthyl)ethylamine (NEA)/Cu(111).<sup>10</sup> This we attribute to the more heterogeneous nature of solution-deposited SAMs, which contain domains of a variety of structures, some of which may not chirally perturb the underlying electronic structure.

**Is the Induction of Optical Activity in Nanoparticles and Extended Films Linked?** Intuitively, one would suspect that there is a link between the induction of optical activity in nanoscale Au films and the chiroptical behavior of Au and Ag nanoparticles; this assumption is reinforced by the observation that COOH groups<sup>2–7</sup> facilitate the induction of optical activity in both cases. A caveat should be placed on any comparison between nanoparticles and extended films, and that is the adsorption structures of cysteine in the two cases may differ. However, experimental evidence suggests that the adsorption geometry of cysteine does not differ significantly between nanoparticles<sup>4</sup> and extended surfaces.<sup>24</sup> In both cases a chemisorbed Au–S bond is formed, the NH<sub>2</sub> points toward and the COOH groups points away from the surface. Three mechanisms have been proposed to rationalize the origin of the observed optical activity of chiral thiol-protected nanoparticles; they are:

- chiral induction without physical distortion,
- chiral reconstruction of the nanoparticle, and
- intrinsic chirality of the nanoparticle.

The foundation for the postulation of mechanism iii is theoretical work that indicates that small metal particles such as Au<sub>28</sub> prefer low-symmetry chiral structures over high-symmetry achiral structures.<sup>26</sup> Chiral protecting groups then make the formation of one of the enantiomers of the clusters more favorable. The results of the current study would suggest mechanism ii is responsible, and that the electronic structure of an achiral nanoparticle could be chirally perturbed by the presence of a cysteine or a cysteine derivative, and that there is no need for the particle to be intrinsically chiral to display optical activity. The most important factor that would influence the induction of optical activity is ordering, facilitated by intermolecular H-bonding, of the chiral thiol protecting groups. The size dependence of the optical activity of nanoparticles, it decreases with increasing particle size, can then be understood in terms of the relative contribution of the surface region to

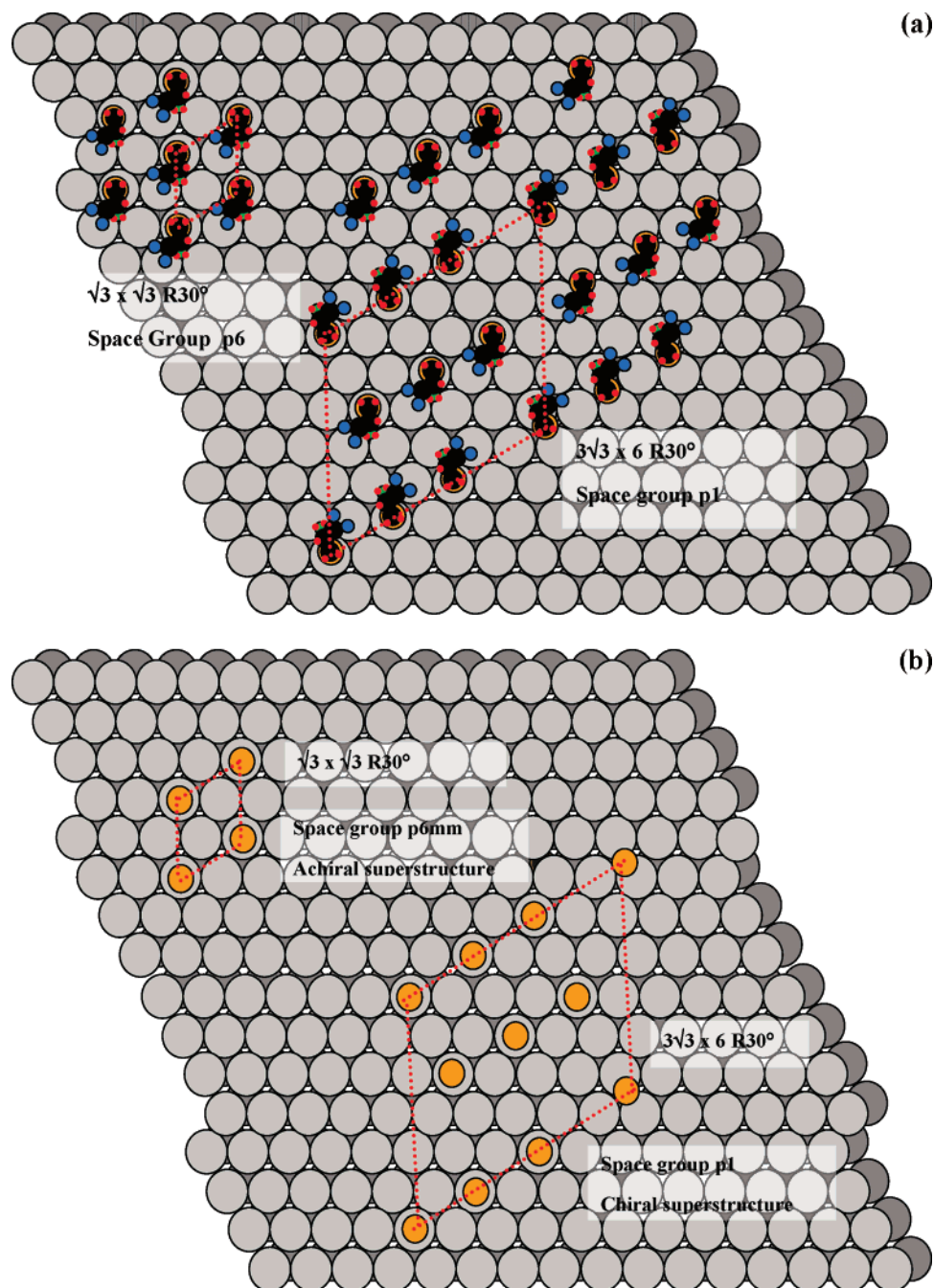


**Figure 7.** (a) Diagram (not to scale) illustrating the  $\sqrt{3} \times \sqrt{3} R30^\circ$  and  $3\sqrt{3} \times 6 R30^\circ$ . (b) The “footprints” of both structures are shown. The unit cells of each of the structures has been highlighted.

overall (bulk + surface) electronic structure decreasing with increasing particle size.

### Summary

We have demonstrated that the adsorption of both cysteine and penicillamine can induce chiral electronic states in an initially achiral Au surface. From the pH dependence of the induction of the chiral perturbation we have demonstrated that the induction of a chiral perturbation on the surface electronic structure is facilitated by hydrogen-bond-mediated supramolecular assembly of the adsorbed moieties. Such supramolecular assembly generates ordered overlayers with oblique Bravais lattice. The chiral induction is not associated with the local structure of the adsorbed moiety but is, rather, associated with the chiral footprint displayed by the extended structure.

**Acknowledgment.** We acknowledge the EPSRC for funding and Dr. A. Sutherland for help with sample preparation and useful discussions.

**Supporting Information Available:** C(1s) and S(2p) XPS data collected from cysteine layers deposited under acidic conditions. This material is available free of charge via the Internet at <http://pubs.acs.org>.

### References and Notes

- (1) Shriver, D. F.; Atkins, P. W.; Langford, C. H. *Inorganic Chemistry*, 2nd ed.; Oxford University Press: Oxford, 1994.
- (2) Schaaf, G. T.; Whetten, R. L. *J. Phys. Chem. B* **2000**, *104*, 2630.
- (3) Yao, H.; Miki, K.; Sasaki, A.; Kimura, K. *J. Am. Chem. Soc.* **2005**, *127*, 15536.
- (4) Gautier, C.; Bürgi, T. *J. Am. Chem. Soc.* **2006**, *128*, 11079.
- (5) Li, T.; Park, H. G.; Choi, S. H. *Nanotechnology* **2004**, *15*, S660.



- (6) Shemer, G.; Krichevski, M. G.; Molotsky, T.; Lubitz, I.; Kotlyar, A. B. *J. Am. Chem. Soc.* **2006**, *128*, 11006.
- (7) Yanagimoto, Y.; Negishi, Y.; Fujihara, H.; Tsukuda, T. *J. Phys. Chem. B* **2006**, *110*, 11611.
- (8) Petty, J. T.; Zheng, J.; Hud, N. V.; Dickson, R. M. *J. Am. Chem. Soc.* **2004**, *126*, 5207.
- (9) Mulligan, A.; Lane, I.; Rousseau, G. B. D.; Johnston, S. M.; Lennon, D.; Kadodwala, M. *Angew. Chem., Int. Ed.* **2005**, *44*, 1830.
- (10) Mulligan, A.; Lane, I.; Rousseau, G. B. D.; Johnston, S. M.; Lennon, D.; Kadodwala, M. *J. Phys. Chem. B* **2006**, *110*, 1083.
- (11) Mulligan, A.; Lane, I.; Rousseau, G. B. D.; Johnston, S. M.; Hecht, L.; Lennon, D.; Kadodwala, M. *Chem. Commun.* **2004**, 2492.
- (12) de la Fuente, J. M.; Andar, A.; Gadegaard, N.; Berry, C. C.; Kingshott, P.; Riehle, M. O. *Langmuir* **2006**, *22*, 2156.
- (13) Bourguignon, B.; Zheng, W.; Carrez, S.; Fournier, F.; Gaillard, M. L.; Dubost, H. *Surf. Sci.* **2002**, *515*, 567.
- (14) Wang, E. K. L.; Richmond, G. C. *J. Chem. Phys.* **1993**, *99*, 5500.
- (15) Schwab, C.; Meister, G.; Woll, J.; Gerlach, A.; Goldmann, A. *Surf. Sci.* **2000**, *457*, 273.
- (16) Buck, M.; Grunze, M.; Eisert, F.; Fischer, J.; Trager, F. *J. Vac. Sci. Technol., A* **1992**, *10*, 926.
- (17) Ihs, A.; Liedberg, B. *J. Colloid Interface Sci.* **1991**, *144*, 282.
- (18) Gonella, G.; Terreni, S.; Cvetko, D.; Cossaro, A.; Mattera, L.; Cavalleri, O.; Rolandi, R.; Morgante, A.; Floreano, L.; Canepa, M. *J. Phys. Chem. B* **2005**, *105*, 18003.
- (19) Schrieber, F. *J. Phys.: Condens. Matter* **2004**, *16*, R881.
- (20) Yu, M.; Bovet, N.; Satterley, C. J.; Bengio, S.; Lovelock, K. R. J.; Milligan, P. K.; Jones, R. G.; Woodruff, D. P.; Dhanak, V. *Phys. Rev. Lett.* **2006**, *97*, 166102.
- (21) Dakkouri, A. S.; Kolb, D. M.; Edelstein-Shima, R.; Mandler, D. *Langmuir* **1996**, *12*, 2849.
- (22) Zhang, J.; Chi, Q.; Neilsen, J. U.; Friis, E. P.; Andersen, J. E. T.; Ulstrup, J. *Langmuir* **2000**, *16*, 7229.
- (23) Xu, Q. M.; Wan, L. J.; Wang, C.; Bai, C. L.; Wang, Z. Y.; Nozawa, T. *Langmuir* **2001**, *17*, 6203.
- (24) Kuhnle, A.; Linderroth, T. R.; Schunack, M.; Besenbacher, F. *Langmuir* **2006**, *22*, 2156.
- (25) Nazmutdinov, R. R.; Zhang, J.; Zinkicheva, T. T.; Manyurov, I. R.; Ulstrup, J. *Langmuir* **2006**, *22*, 7556.
- (26) Roman-Velazquez, C. E.; Noguez, C.; Garzon, I. L. *J. Phys. Chem. B* **2003**, *107*, 12035.